

The Hardness Distribution of Gamma-Ray Bursts

Ehud Cohen, Tsvi Piran

Racah Institute of Physics, The Hebrew University, Jerusalem 91904, Israel

and

Ramesh Narayan

Harvard-Smithsonian Center for Astrophysics, Cambridge, MA 02138, U.S.A.

ABSTRACT

It is often stated that gamma-ray bursts (GRBs) have typical energies of several hundreds keV, where the typical energy may be characterized by the hardness H , the photon energy corresponding to the peak of νF_ν . Among the 54 BATSE bursts analyzed by Band et al. (1993), and 136 analyzed by us, more than 60% have $50\text{keV} < H < 300\text{keV}$. Is the narrow range of H a real feature of GRBs or is it due to an observational difficulty to detect harder bursts? We consider a population of standard candle bursts with a hardness distribution: $\rho(H)d\log H \propto H^\gamma d\log H$ and no luminosity - hardness correlation. We model the detection algorithm of BATSE as a function of H , including cosmological effects, detector characteristics and triggering procedure, and we calculate the expected distribution of H in the observed sample for various values of γ . Both samples shows a paucity of soft (X-ray) bursts, which may be real. However, we find that the observed samples are consistent with a distribution above $H = 120\text{keV}$ with $\gamma \sim -0.5$ (a slowly decreasing numbers of GRBs per decade of hardness). Thus, we suggest that a large population of unobserved hard gamma-ray bursts may exist.

Subject headings: gamma rays: bursts

1. Introduction

One striking feature that is common to all gamma-ray bursts (GRBs) is the fact that most of the observed photons correspond to low energy gamma-rays, with energies of a few tens to few hundreds of keV. While other features of the bursts, in particularly the temporal structure, vary significantly from one burst to another, this feature seems to be quite invariant. One wonders, therefore, whether this is a clue to the nature of GRBs - a phenomenon that theorists should strive to explain - or if it is just a consequence of an observational bias against detection of harder or softer bursts. In other words, one can ask whether the observed hardness distribution represents the real one.

Piran & Narayan (1995) have assumed a simple model for the sources and the detector, and used a sample of 54 relatively strong bursts analyzed by Band et. al. (1993), to find out if GRBs have intrinsic hardness values around 100 – 400keV, or the observed distribution is just a data selection effect. They have found that the intrinsic hardness distribution can be extended to include hard bursts with no upper limit.

We calculate the expected observed hardness distribution for several intrinsic hardness distributions. The calculations include cosmological red-shift and detector characteristics. We calculate the observed hardness distribution of a set of 136 bursts and we compare the theoretical distribution to the observed one. We examine which intrinsic distributions are consistent with the data and which are not.

In section 2 we describe our data set, the method used for estimating the spectra and the resulting hardness distribution. In section 3 we calculate the expected observed hardness distribution from a given intrinsic distribution. As our calculations deal with cosmological effects on the hardness distribution, we include in section 4 a discussion of the possible correlation between intensity and hardness of cosmological bursts. Finally, in section 5 we discuss the constrains imposed on the intrinsic distribution by the observed data.

2. The Observed Hardness Distribution

2.1. Data

Using a count spectrum averaged over the estimated total duration interval for each event, we calculate the photon energy spectra for a group of GRBs using the MER/CONT data from BATSE Large Area Detectors. These data consist of count rates in 16 energy channels spanning a range of approximately 20 – 2000keV, with different temporal

resolutions. To estimate the bursts' spectra we must subtract the background. This background was fitted with a polynomial of order one or two on intervals before and after the burst (Nemiroff 1995).

We limit our sample to bursts that occurred before November 1991 and between February 1992 and January 1993. We consider bursts with a minimal peak-flux condition ($flux_{256} > 0.5 \text{ ph cm}^{-2}\text{s}^{-1}$) and require the availability of flux measurements in the 256msec, counts in the 1024msec channel and an estimate of the burst duration. We consider only bursts that have continuous data for all the duration of the burst, (the data dropouts is due to telemetry conditions and has no relation to the bursts' data, we expect, therefore, that this sample is a proper sample of the GRB population.). A total of 136 bursts satisfy these conditions.

2.2. The Intrinsic Spectrum

The BATSEs' LAD detector estimates the energy of incident photons. However, due to various detector characteristics (Pendelton et. al. 1995), there is no one to one correspondence between the true energy of the photon and the measured one. The BATSE team provides for each burst a *DRM* matrix which describes the detector response to photons at various energies, i.e.

$$C = DRM * P, \tag{1}$$

where P is the incident photon spectra (vector length is 62), DRM is the detector response matrix (size 16*62) and C is the count spectra (a vector of length 16).

The counts spectra must be transformed into a photon spectra. A direct inversion is impossible as it is well known that the inverse matrix is singular. We have used the forward folding method. This is a model dependent method. One assumes that the photon spectra is well described by a given functional shape with some unknown parameters, (we have used the Band parameterization). For a given set of parameters, the assumed spectral form is integrated into the *DRM* spacing, multiplied by the *DRM*, and compared with the measured count vector. Then, we use the χ^2 optimization method to find the parameters that fit best the measured count vector.

2.3. The Band Spectrum

With the necessity of assuming a spectral form, we follow Band et. al. (1993), by characterizing the bursts' spectra using a four parameter function:

$$N_P(E)dE = \begin{cases} A/100\text{keV} [E/100\text{keV}]^\alpha e^{-E/E_0} & E < (\alpha - \beta)E_0 \\ A/100\text{keV} [(\alpha - \beta)E_0/100\text{keV}]^{\alpha-\beta} e^{\beta-\alpha} [E/100\text{keV}]^\beta & E > (\alpha - \beta)E_0 \end{cases} \quad (2)$$

This function, which provides a good fit to most of the observed spectra, is characterized by two power laws joined smoothly at a break energy $(\alpha - \beta)E_0$. For most of the observed values of α and β , $\nu F_\nu \propto E^2 N(E)$ rises below $H = (\alpha + 2)E_0$, and decrease above it. The energy H is thus the “typical” energy of the observed burst. Note that the hardness ratio in BATSE catalogue, which is the ratio of photons observed in channel 3 to those observed in channel 2, is different from H defined in this way.

The total energy of a burst described by this spectral form depends on the hardness of the burst, and on its power-law slopes. Using $\gamma(a > 0, x) = \int_0^x e^{-t} t^{a-1} dt$, we calculate the total energy of a burst

$$E_{TOT} = \int_0^\infty EN_P(E)dE = AE_0 \left(\frac{E_0}{100\text{keV}}\right)^{\alpha+1} \left[\gamma(\alpha + 2, \alpha - \beta) - (\alpha - \beta)^{\alpha+2} e^{\beta-\alpha} / (\beta + 2)\right]. \quad (3)$$

The observed hardness distribution of our sample appears in Fig. 1 together with the hardness distribution of the sample of Band et. al. (1993). Fig 2. shows the distribution of the lower energy power-law parameter α . We use the total duration of the bursts to produce photon spectra. The known hard to soft evolution causes the hardness distribution to be softer then the hardness distribution at the peak of the bursts, which is needed for detection statistics. We ignore this effect. Inclusion of it will make the intrinsic hardness distribution even harder than our estimates.

3. The Theoretical Model

To calculate a theoretical “observed” hardness distribution, we must assume a model for the hardness intensity statistics of the sources. For simplicity, we assume: (i) Standard candle in peak energy flux, (ii) No hardness vs. intensity correlation. We believe that this is the simplest possible ad-hoc model. One can easily imagine physical processes that will lead to this situation. For example, within the relativistic fireball model (Piran 1996) such a behavior will arise if we keep the total energy of the fireball fixed and vary the Lorentz factor of the relativistic motion. (iii) We also assume a simple form of the intrinsic hardness

distribution:

$$\rho(H)d \log H = \begin{cases} 0 & H \leq H_{min}, H \geq H_{max} \\ H^\gamma & H_{max} > H > H_{min} \end{cases}, \quad (4)$$

where the index γ is such that if $\gamma = 0$ there are equal number of bursts per logarithmic interval of H between H_{min} and H_{max} . If $\gamma > 0$, then there are more hard bursts than soft ones. We also assume that for all bursts $\bar{\alpha} = -0.65$ and $\bar{\beta} = -2.6$ which are the average values of our sample. (Later, after we find the intrinsic hardness distribution which fits the observed data the best, we check the sensitivity to a distribution of power-law indices. See section 3.3).

In order to produce a set of bursts with the same total energy we calibrate the spectra by setting the constant A in equation 3 to hold $E_{TOT} = Const.$ fixed for all the bursts.

We calculate the distribution of observed hardness, which is

$$N(H_{obs})d \log H = \int_{H_{min}/\min(H_{obs}, H_{min})-1}^{H_{max}/H_{obs}-1} n(z)\rho[H_{obs}(1+z)]\Psi(z)dz, \quad (5)$$

where $n_z(z) = 16\pi(c/H_0)^3(\sqrt{1+z}-1)^2(1+z)^{-7/2}dz$ is the proper volume of a shell extending from z to $z+dz$, compensated for event count rate, assuming constant rate of GRBs per proper time per comoving volume and $\Omega = 1$. The detection function $\Psi(z)$ states if the burst with hardness $H_{obs}(1+z)$ is observable with our detector. The main BATSE triggering algorithm uses only counts in the region $50\text{keV} < E < 300\text{keV}$ (cf. discussion in section 3.2). With these assumptions,

$$\Psi(z; H_{obs}) = \Theta \{C_{50-300}[H_{obs}(1+z), \alpha, \beta, z] - C_{min}\}, \quad (6)$$

where $C_{50-300}(H, \alpha, \beta, z)$ is the peak rate of photons the detector receives from a source at red-shift z in the interval $50\text{keV} - 300\text{keV}$ (the BATSE detection window) at 1024msec. The 50keV to 300keV range (channels 2 & 3 of BATSE) is a feature of the BATSE triggering algorithm. Clearly a triggering algorithm based on different BATSE channels will result in different data selection effects. The sources are normalized as standard candles in peak luminosity using equation 3. For simplicity we use a fixed count threshold, C_{min} . We then use the χ^2 method to find which parameters $(H_{min}, H_{max}, \gamma)$ fits the observed distribution the best.

The best fit parameter for our data set are $H_{min} = 120\text{keV}, \gamma = -0.5$. The upper cut-off of the hardness distribution, H_{max} is not constrained by current data. This intrinsic hardness distributions agrees with Piran & Narayan (1995), in that the observed hardness distribution is compatible with a large number of non-detectable MeV bursts, and the apparent upper-cut off arises from data selection effects.

3.1. Data selection effects.

It is interesting to check whether one can overcome the data selection effects by modifying the triggering algorithm, or are the selection effects inherent triggering algorithm that depends on counts. We model three different possible algorithms, based on different photon energy ranges: (i) 50-300 keV (currently the main BATSE algorithm) (ii) 50-2000 keV and (iii) 300-2000 keV. We assume that the hardness distribution is given by Eq. 4 with $\gamma = -.5$ and $H_{min} = 120$ keV. We also assume that the spectrum for the underlying noise behaves like $\nu F_\nu = const.$ We calculate the distribution of hardness expected with this intrinsic distribution and these three different triggering algorithms (see Fig. 2). We find that inclusion of the the 300-2000keV channel increases the overall rate of observed bursts by 12% compared to triggering on the 50-300 keV alone. Using only the 300-2000keV leads to a decrease in the total rate by 10% (this last number depends rather sensitively on the lower cut off chosen in the intrinsic hardness distribution). What is more important is that even while triggering on the 300-2000 keV photons, there is still a large difference between the observed distribution and the intrinsic one (see Fig. 2). This shows that the inherent problem in detecting harder bursts is the decrease in the total number of photons as the hardness increases which is not compensated by an equivalent decrease in the noise.

3.2. Detector Characteristics

The Detector Response Matrix translates the spectrum of incident photons to the measured spectrum of counts. (see section 2.2). The function $C_{50-300}(H, \alpha, \beta, z)$ in eq. 6 ignores the DRM and uses instead the identity matrix. In order to check this effect, we take an arbitrary DRM (burst 3B920226) and define a modified count function

$$\tilde{C}_{50-300}(H, \alpha, \beta, z) = \sum_{i,k} DRM_{i,k} \cdot C_{\nu_i-\nu_{i+1}}(H, \alpha, \beta, z), \quad (7)$$

where ν_i are the DRM photon spectra boundaries, and k spans all the count channels with energies from 50 keV to 300 keV. In table 1 we show the DRM effect on counts, for bursts with various hardnesses. Using this modified count function, we recalculated eq. 5. A sample $N(H)$ distribution (see Fig. 1), with DRM inclusion, shows increasing number of hard bursts which results from hard photons that are measured as softer ones. We see that this effect does not change the distribution significantly.

3.3. Spectral diversity

The spectral shape of a burst in the low energy regime, i.e. the power-law parameter α , can determine if the detector detects the burst or not, even if the hardness is constant. A hard burst with average α might not be detectable. A burst with the same hardness but lower α , has more photon in the detector window, and can be detected. Piran & Narayan (1995) found a negative correlation between hardness and the parameter α , which can be explained by this effect. We proceed to evaluate the sensitivity of our previous calculation to diversity in α . We calculate the expected observed hardness distribution for intrinsic hardness distribution and intrinsic distribution of the α , where for the later we take the observed one (see Fig. 3). It appears from Fig. 1, that the modified hardness distribution is slightly softer, which can be explained by the population of bursts with a higher α than the average one. We find that this spectral diversity does not change our results significantly.

4. Correlations

It is generally assumed that positive correlation between fluence and hardness should appear if the bursts are cosmological. However, while looking for this correlation one should beware of correlating between parameters which have an inherent correlation induced by their estimation method (Schaefer 1993).

For example, assuming that α & β are constants for all bursts, equation 3 becomes $F \propto N \cdot H$, where F is the fluence, N is the photon count, and H is the bursts' hardness. Assuming that there is no intrinsic correlation between the photon counts and hardness, and that the distribution function are "well behaved", we define the spread in hardness and counts by $S_H = Var(H)/\langle H \rangle^2$ and $S_N = Var(N)/\langle N \rangle^2$ respectively. Then the correlation coefficient between fluence and hardness is

$$r = \frac{\sum_i (N_i H_i - \langle NH \rangle)(H_i - \langle H \rangle)}{\sqrt{\sum_i (N_i H_i - \langle NH \rangle)^2 \sum_i (H_i - \langle H \rangle)^2}} = \sqrt{\frac{S_H}{S_N(1 + S_H) + 1}} > 0. \quad (8)$$

The result depends on the distribution of H and N , but it is always positive, and it can have an arbitrary positive value without any intrinsic correlation.

In the case of standard candles with an intrinsic hardness cosmological effects lead to a one to one relation between counts and observed hardness, and a positive correlation between them is inevitable. However, consider a population of GRBs in a certain red-shift z , with a hardness distribution. The correlation between hardness and counts would be *negative*, because (for standard candles) the harder bursts emit less photons, and even

less photons inside BATSEs’ triggering interval. What should we expect from GRBs which are spread over the universe *and* have an intrinsic hardness distribution? Fig. 4 shows the average hardness as a function of counts for two intrinsic hardness distribution in the form of eq. 4 (We prefer to use counts rather than intensity, due to the usage of the bursts’ spectra while calculating its’ intensity (Pendelton et. al. 1996)). Both curves are for a constant number of GRBs per logarithmic hardness interval. The descending curve corresponds to hardness distribution with $H_{min} = 100\text{keV}$ and $H_{max} = \infty$, and the ascending curve to hardness distribution with $H_{min} = 100\text{keV}$ and $H_{max} = 500\text{keV}$. It is easy to see that even a mild hardness distribution masks cosmological effects (recall that a hardness distribution with $H_{min} = 100\text{keV}$ and $H_{max} = 500\text{keV}$ is too narrow to fit the observed one). Thus, the large observed hardness distribution disables the usage of hardness-intensity relation as an independent probe for the bursts’ cosmological origin.

We find a correlation coefficient smaller than 2×10^{-2} between hardness and peak flux. This result agrees with Band et. al. (1993) who have found a correlation coefficient of -8×10^{-2} . Mallozzi et. al. (1995) have found a marginally significant correlation (0.9). In Fig. 5 we compare the hardness - intensity relation in our and Mallozzi et. al. (1995) samples. The intensity is the peak flux in 256msec channel from BATSEs’ catalog. It is not clear if the two data sets are discrepant or not. This warrants further investigations.

5. Discussion and Conclusions

A comparison between the expected hardness distribution for various intrinsic hardness distributions, and the observed distribution reveals the necessity for intrinsic paucity of soft bursts. Any intrinsic distribution, that does not include an intrinsic paucity in this area, does not fit the observed distribution. Therefore, unless BATSE has an unexpected and unknown selection bias against soft photons, the lower cut-off in the observed distribution is a real phenomenon. Using a best fit method, we found that the observed data is best modeled by intrinsic lower cut-off at 120keV.

The story is, however, very different for large values of H. The data show very small numbers of hard bursts, e.g., only two bursts out of 54 bursts in the Band et. al. (1993) sample and only five bursts out of 136 in our sample are harder than 1 MeV. Nevertheless, this does not mean that there are fewer GRBs above 1 MeV. The best fitted intrinsic hardness distribution, is one with $\gamma = -0.5$, i.e. a slowly decreasing number of bursts per logarithmic interval. Even a model with $\gamma = 0$, i.e. a constant number of bursts per logarithmic hardness interval gives a probability of 15% in a KS test, which is not high but is not sufficiently low to rule out the model.

The interpretation of the result is quite simple. There is an observational bias against detecting bursts with $H \geq 500\text{keV}$ by current detectors. Two factors operate. For bursts with a fixed luminosity, harder bursts have fewer photons. This makes the detection of harder bursts difficult in any detector that is triggered by photon counts. (If the energy of the detector noise per decade is constant, then the the ratio between the number of photons in the burst and in the noise remains constant. However, the noise variance decreases slowly with energy (square-root of the total noise), and the signal to noise decreases.) The decrease in sensitivity in BATSE is even more severe since BATSE triggers on photons in the 50keV to 300keV range and as the bursts become harder most of the emitted photons are further and further away from this energy range. A careful comparison between the hardness distributions observed with different triggering algorithms in BATSE 4B catalog might give some indication on the high energy hardness distribution.

6. Acknowledgments

We thank D. Band for helpful discussions. This research was supported by a US-Israel BSF grant 95-238 and by a NASA grant NAG5-3516.

REFERENCES

- Band, D., et. al. 1993, ApJ, 413, 281
- Mallozi, R. S., et. al. 1995, ApJ, 454, 597
- Nemiroff, B. 1995, private communication
- Pendelton, G.N. et. al. 1995, preprint
- Pendelton, G.N. et. al. 1996, ApJ, 464, 606
- Piran, T., & Narayan, R., 1995 in GRB 3'rd Huntsville Symposium, Eds. C. Kouveliotou, M. F. Briggs & G. J. Fishman (AIP)
- Piran, T., 1996, in *Some Unsolved Problems in Astrophysics*, Eds. J. N. Bahcall and J. P. Ostriker, Princeton University Press.
- Schaefer, B. E., 1993, ApJ, 404, L87

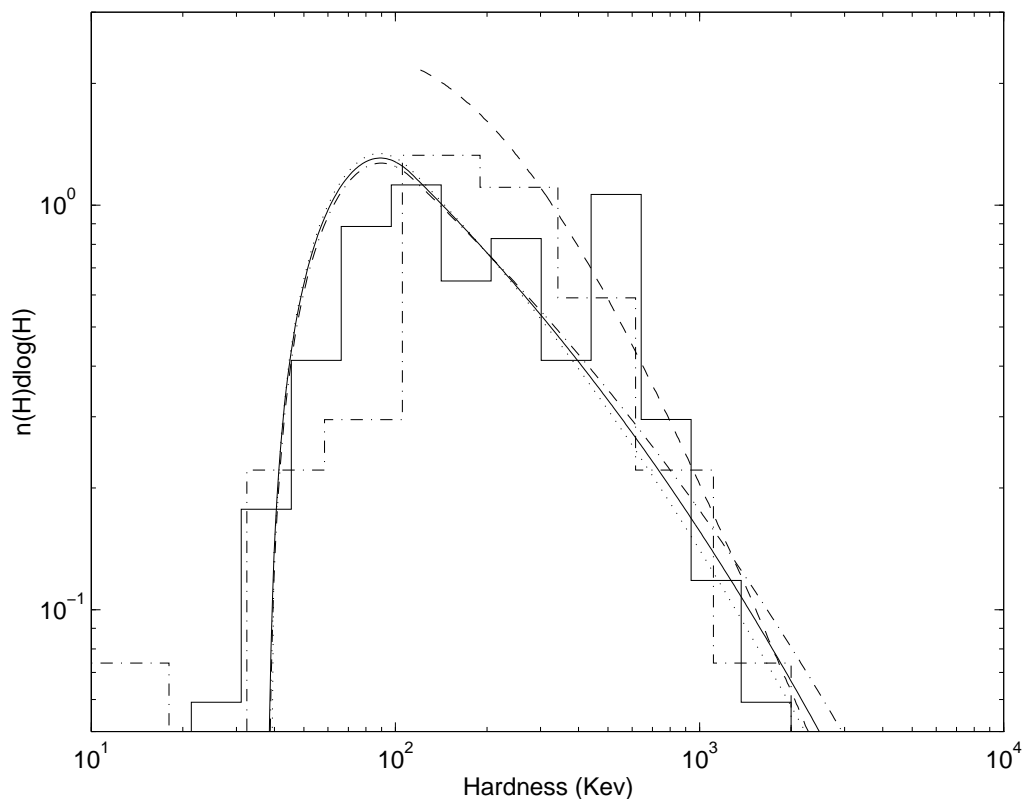


Fig. 1.— The observed hardness distribution for Band et. al. (1993) sample (dashed-dotted) and our sample (solid), imposed on expected hardness distribution for intrinsic hardness distribution with $\gamma = -0.5, H_{min} = 120\text{keV}$ (solid line). The dashed-dotted curve includes effects of a DRM, and the dotted curve includes a diversity in the spectral parameter α . The dashed line corresponds to a hardness distribution with $\gamma = 0, H_{min} = 120\text{keV}$, neglecting cosmological effects.

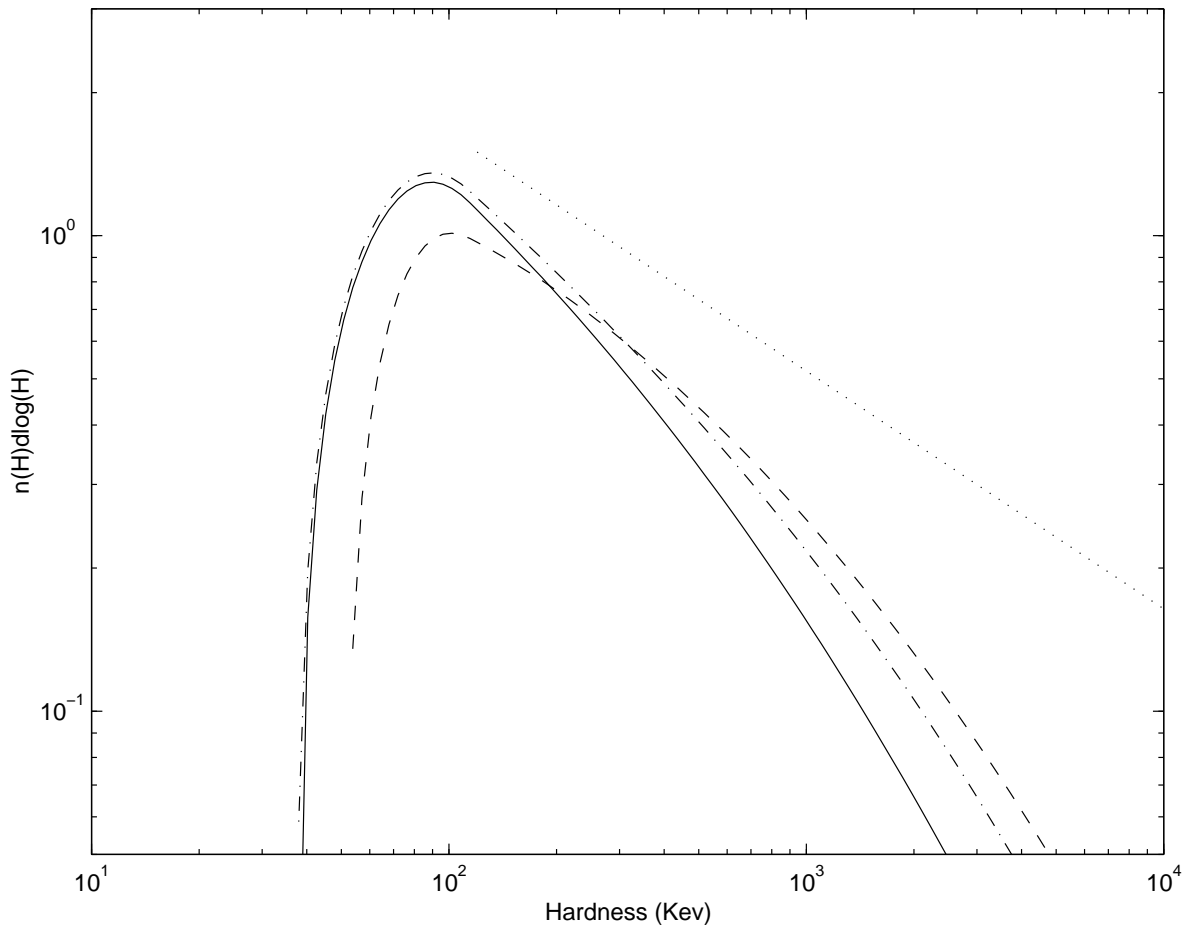


Fig. 2.— The expected observed hardness distribution for different triggering mechanism, assuming an intrinsic hardness distribution with $\gamma = -0.5, H_{min} = 120\text{keV}$ (un-normalized dotted line). The different lines correspond to triggering on 50-300 keV (solid), 50-2000 keV (dashed-dotted) and 300-2000 keV (dashed).

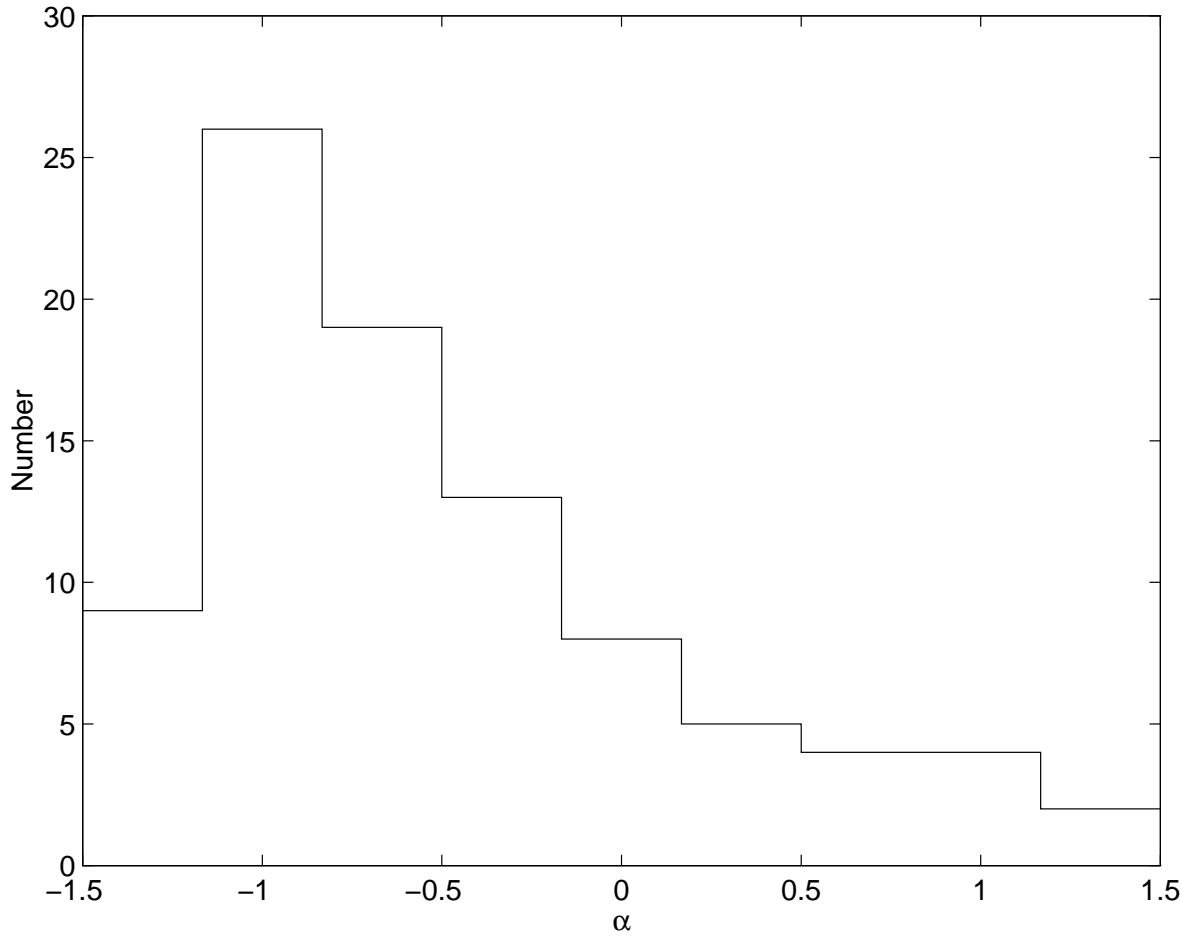


Fig. 3.— The observed distribution of the lower energy power-law parameter α .

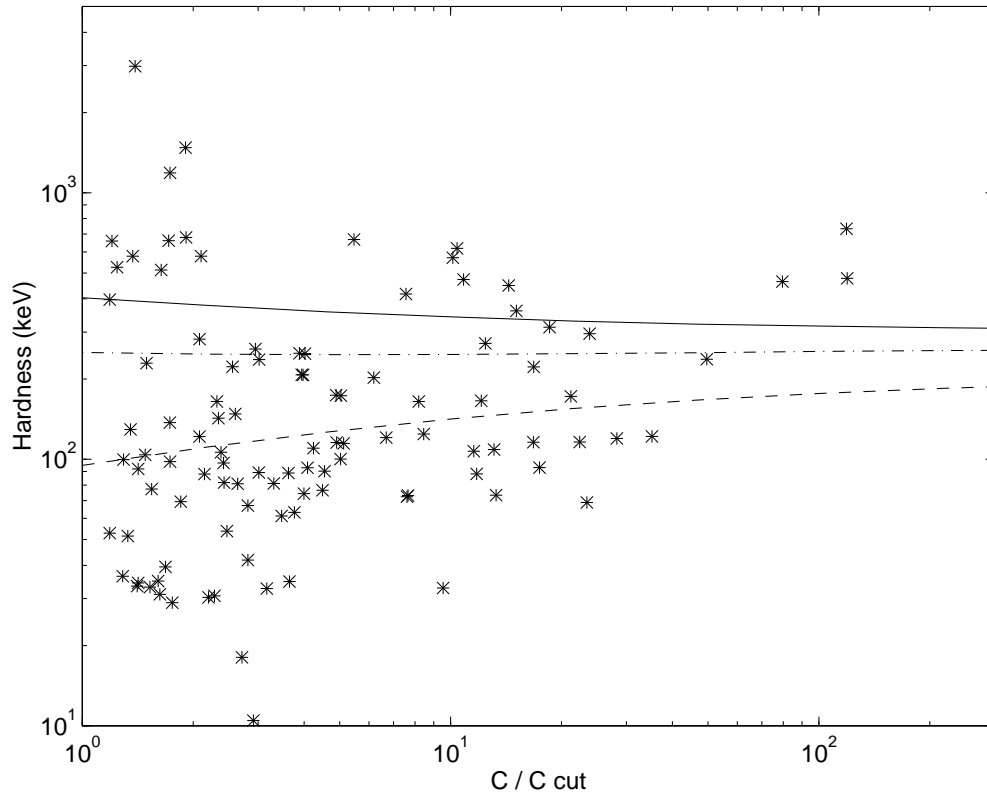


Fig. 4.— The observed hardness vs. counts distribution, with the theoretical curves for a constant number of GRBs per decade of hardness with lower cut off only (solid), with lower and upper cut off (dashed) and the best fit model ($\gamma = -0.5, H_{min} = 120\text{keV}$) (dashed-dotted). The counts are in the 1024msec channel, and $C_{cut} = 289$.

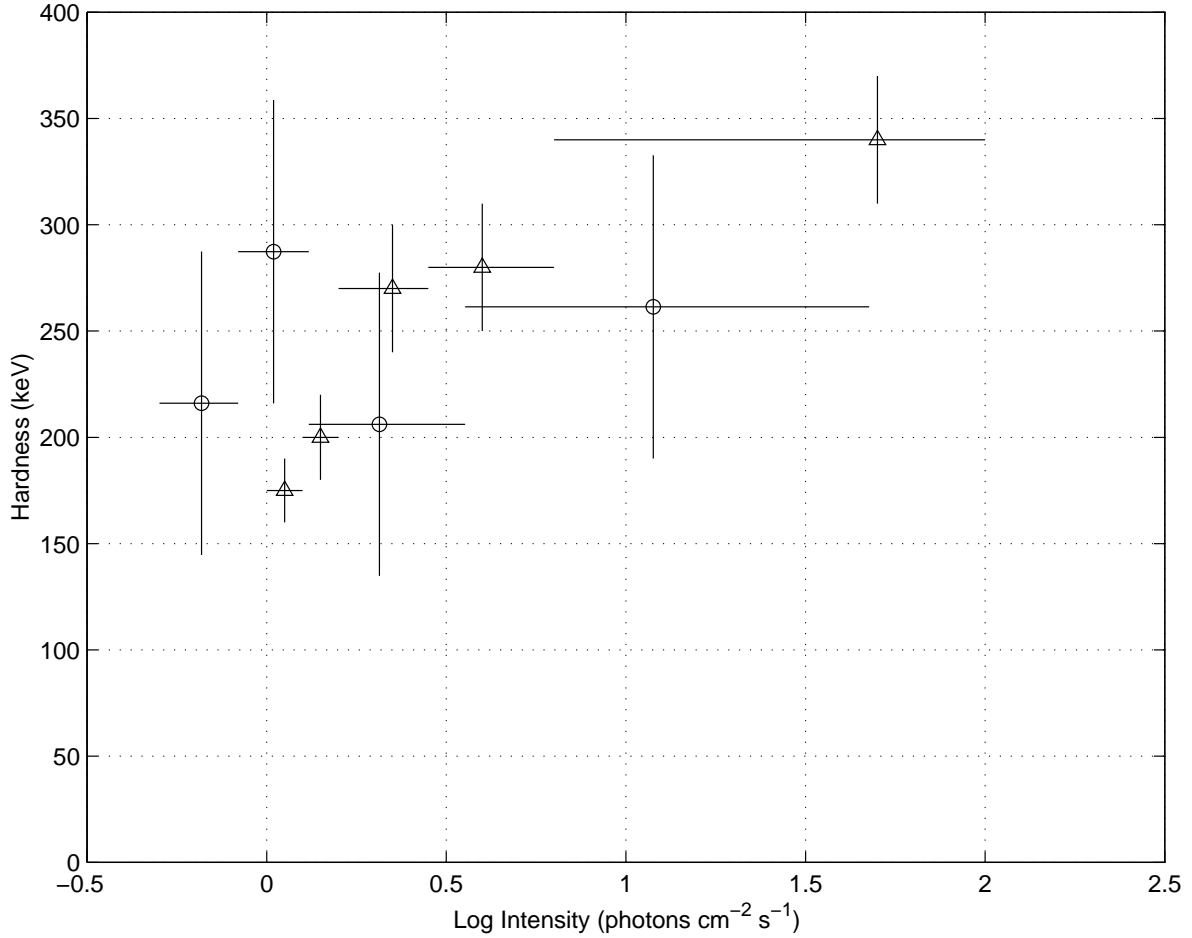


Fig. 5.— The average νF_ν peak energies as a function of intensity (BATSEs’ peak flux) for our results (circles) and Mallozzi et. al. (1995) (triangles). While one sample shows an increasing trend, the other one does not. Still with the large error bars the two samples seems to be consistent.

Table 1. DRM effects - Normalized counts for bursts with various spectra.

Hardness ^a (keV)	Counts < 300keV ^b	Counts > 300keV ^c	Total counts
100.00	93.75	6.25	100.00
500.00	35.99	9.23	45.22
1000.00	17.63	7.13	24.77
1500.00	11.16	5.50	16.66
2000.00	7.97	4.41	12.38

^aPeak of $\nu F\nu$. All bursts spectrum have the same total energy with $\bar{\alpha} = -0.65$ and $\bar{\beta} = -2.6$, normalized to give 100 counts for a burst with hardness of 100 keV

^bCounts in the 50-300 keV regime, from photons with energies < 300 keV.

^cCounts in the 50-300 keV regime, from photons with energies > 300 keV.